

# Toughened Blends of Polystyrene and Polybutadiene Filled with Chalk

D. BRAUN,\* M. KLEIN, and G. P. HELLMANN

Deutsches Kunststoff-Institut, Schlossgartenstrasse 6, D-64289 Darmstadt, Germany

## SYNOPSIS

Brittle thermoplastics are hardened and embrittled by mineral fillers and softened and (sometimes) toughened by elastomers. We investigated the possibility of combining these effects favorably in filled blends of a thermoplastic, polystyrene (PS); an elastomer, polybutadiene (BR); and a filler, chalk. The success had to be measured in comparison to commercial high-impact polystyrene (HIPS) which is produced by *in situ* polymerization. At low concentrations of BR, simple blends of PS/BR are tougher than PS itself, but not considerably. This could be improved by adding chalk. The blends PS/BR/chalk feature a core-shell domain morphology, with BR enveloping chalk aggregates on the micrometer scale. At BR contents of less than 10 vol %, the stress-strain behavior of the filled blends PS/BR/chalk compares well to that of HIPS. The blends exhibit multicrazing with characteristic patterns and can be bent easily without breaking. At higher BR contents, however, the blends go back to brittle failure. © 1996 John Wiley & Sons, Inc.

## INTRODUCTION

Polystyrene (PS) is today a major standard thermoplastic only because ways were found to deal with its brittleness. Usually, PS is either oriented or modified with rubber.<sup>1</sup>

In early attempts to make use of rubber, PS was simply blended with an elastomer. Such blends are toughened to some degree but are still sensitive to impact. The rubber is dispersed, as shown in Figure 1(a), for a blend PS/BR i.e., PS with polybutadiene (BR). The breakthrough for PS came as styrene was polymerized *in situ*, in solutions BR/styrene, which leads to high-impact PS (HIPS).<sup>2-4</sup> HIPS owes its excellent toughness to characteristic "salami" domains, as shown in Figure 1(b). The domains are heavily filled with PS subdomains. The BR, which is mostly converted into a graft copolymer BR-*g*-S, forms thin lamellar microphases that run through

the domains and cover their surfaces. Under tension or impact, the salami domains initiate multicrazing that deforms the PS matrix considerably before it breaks.<sup>5-7</sup>

Morphologies similar to those of HIPS can be produced in blends of thermoplastics and elastomers containing isotropic fillers. This paper discusses the behavior of blends of PS and BR filled with chalk. As do all mineral fillers, chalk hardens thermoplastics<sup>8,9</sup>; while rubber softens them.<sup>10</sup> The question was: would this lead to synergistic effects similar to those that improve HIPS?

## EXPERIMENTAL

The polymers were PS 168N (BASF AG) with weight average molecular weight  $M_w = 330 \times 10^3$  and BR CB 1409 (Hüls AG) with  $M_w = 380 \times 10^3$ . The chalk was SOCAL P3 (Solvay Alkali GmbH) with a specified primary-particle diameter of 0.2  $\mu\text{m}$ . The mixtures were prepared at 200°C in a kneader

\* To whom correspondence should be addressed.

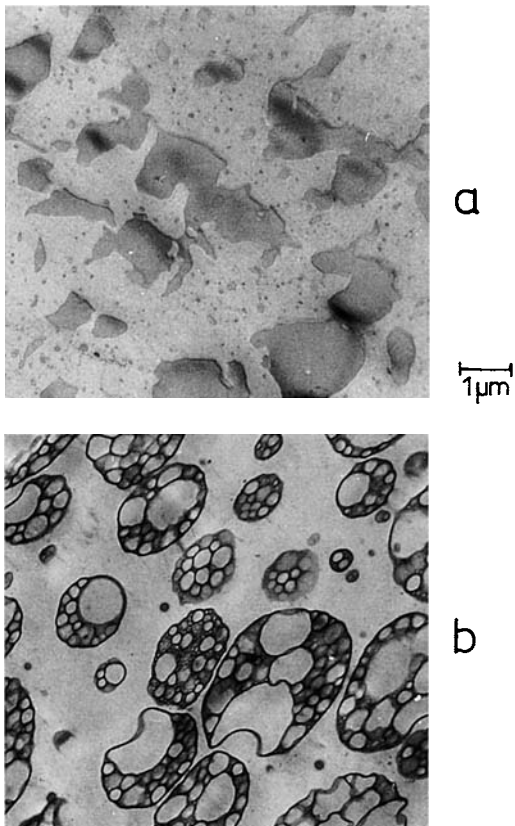


**Figure 1** Characteristic morphologies of (a) blends PS/BR<sub>20 vol %</sub> and (b) HIPS.

(W30H, Plastograph PL35, Brabender GmbH) by adding PS first, then BR, and finally the chalk (10 min mixing, 50 rpm). Reversing the order of BR and chalk or premixing the components in the solid state did not change the results. The HIPS used for comparison was PS 476L containing 10 vol % BR (BASF AG), diluted in the kneader with PS. Tensile (DIN 53455 3/2) and impact (DIN53453) test bars were cut from compression-molded plates. Tensile tests (Zwick 1445) were carried out at a cross-head speed of 2.5 mm/min, and Charpy impact tests (Frank) with a pendulum with 0.5 J. Tensile test bars were also used for bending tests.

The morphology was characterized by transmission electron microscopy (TEM) using ultrathin sections, 80 nm thick, cut at low temperatures (knife, -50°C; sample, -100°C). The chalk particles were cut into slices. Hole formation could be minimized by cutting at high speed. BR domains were contrasted with OsO<sub>4</sub>. Only a moderate contrast was attempted, so the BR domains would remain grey and, therefore, visible in the TEM pictures

between the PS matrix (white) and the chalk particles (black). Crazing was studied in specimens deformed to the brink of breaking, or in broken specimens. For transmission light microscopy (TLM), microsections were used, 20 μm thick and 5 mm

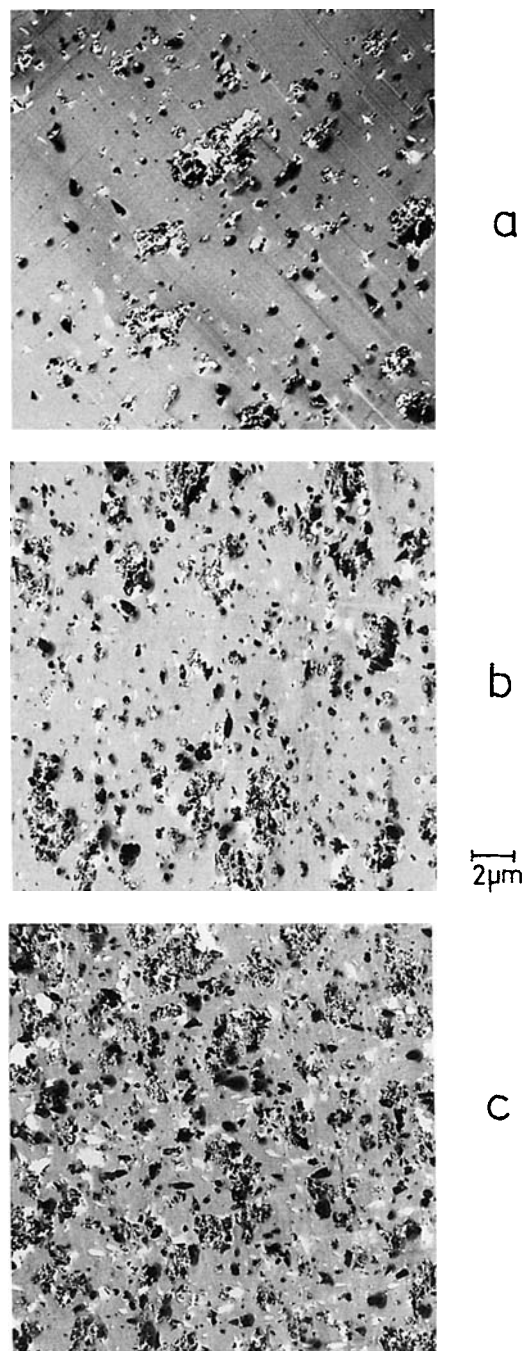


**Figure 2** PS filled with (a) 10, (b) 20, (c) 30 vol % of chalk: primary particles and aggregates.

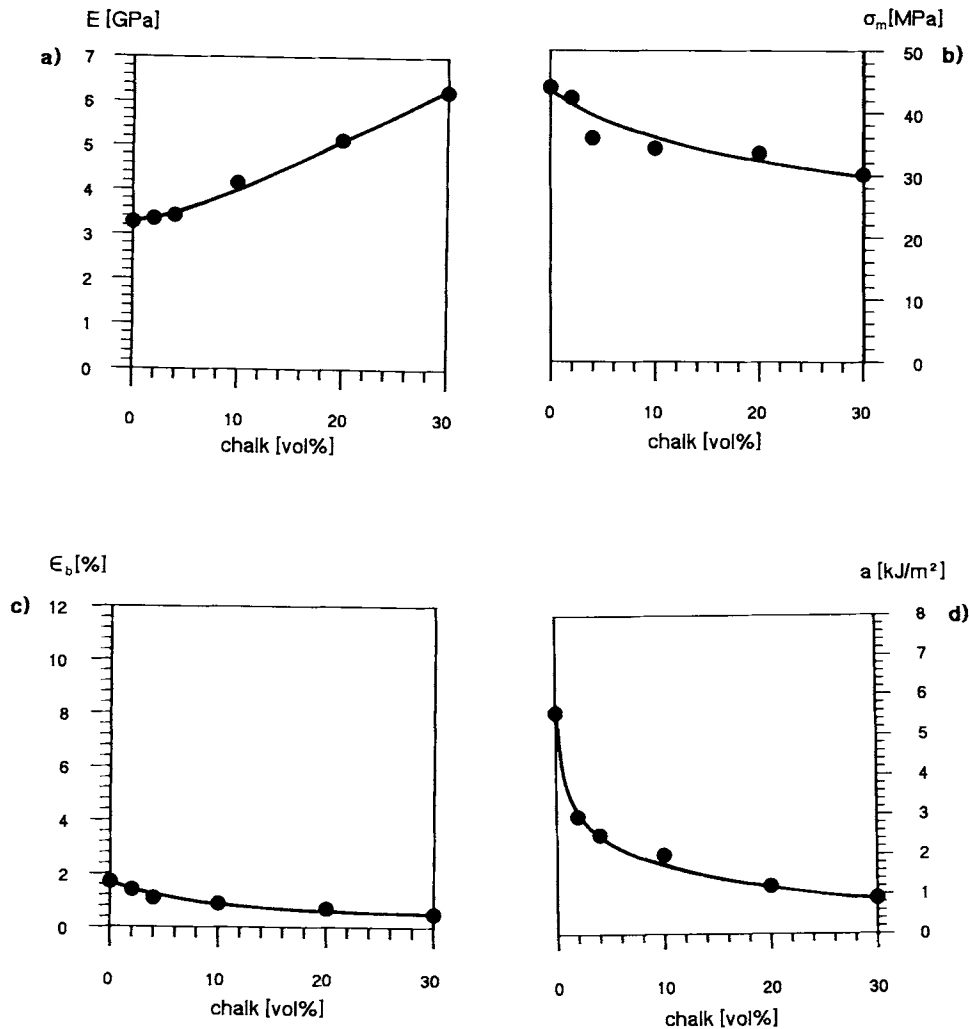


**Figure 3** Filled PS: (a) modulus  $E$ , (b) maximum stress  $\sigma_m$ , (c) elongation at break  $\epsilon_b$ , and (d) impact resistance  $a$ .

square, which were drawn under the microscope. Scanning electron microscopy (SEM) was performed on crazed test bars. Pieces were chipped off the surface and polished. For TEM, ultrathin sections cut from crazed test bars were used. The crazes had to be fixed with  $\text{OsO}_4$ , and had to be cut in-plane; otherwise they were closed by the knife and therefore invisible, or they were torn open and the section was destroyed.

## RESULTS

Three systems were investigated: the ternary system PS/BR/chalk and, for comparison, the binary systems PS/chalk and PS/BR.

### PS/Chalk

TEM of PS filled with chalk yielded the morphologies shown in Figure 2. The chalk is dispersed into its primary particles,  $0.2 \mu\text{m}$  in diameter, and aggregates thereof, with diameters up to  $2 \mu\text{m}$ . The pattern of aggregation was always the same, with and without BR (see Figs. 6 and 7), and even with other matrix polymers.<sup>11</sup>

The ultrathin TEM sections used for Figure 2 are torn in some spots, inside and outside the chalk aggregates. This could have meant that the filled PS was porous, due to incomplete adhesion of the chalk and the PS. Yet, no holes were observed in TEM sections that were cut at extremely low temperatures, meaning that the materials PS and chalk, as

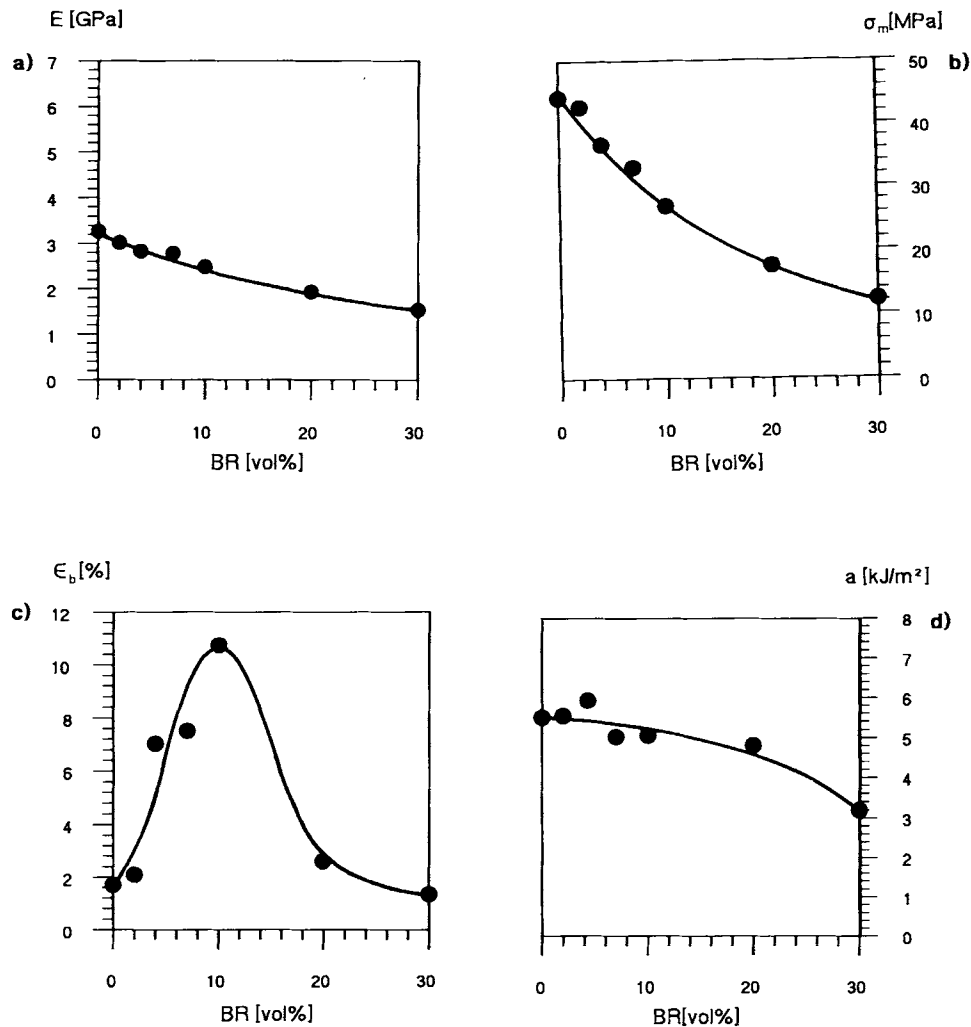


**Figure 4** Unfilled blends PS/BR: (a) modulus  $E$ , (b) maximum stress  $\sigma_m$ , (c) elongation at break  $\epsilon_b$ , and (d) impact resistance  $a$ .

mixed in the kneader, were not porous (at less than 40 vol % chalk). The holes seen in Figure 2 (and in Figs. 6 and 7) were instead produced during the preparation of the TEM sections, by the diamond knife that tears chalk particles and parts of aggregates out of the matrix. In fact, cutting sections at room temperature led to TEM sections with all chalk particles and aggregates torn out.

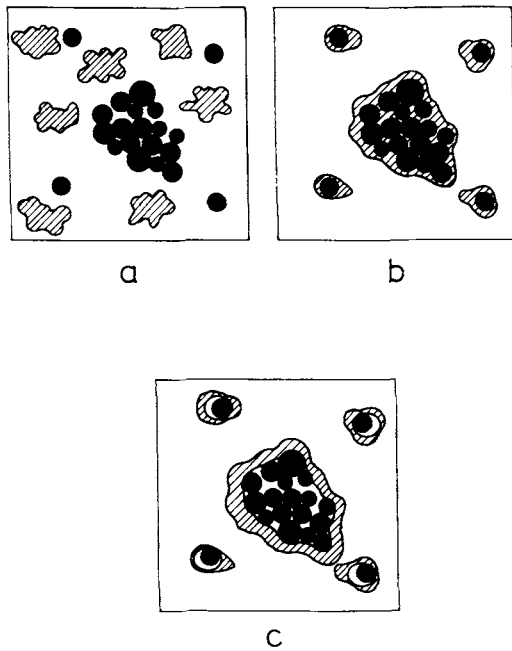
At 40 vol % (corresponding to 61 wt %) and more of chalk, the chalk is more or less densely packed and the PS does not completely fill the intermediate space anymore. This highly filled PS was extremely brittle and, beyond 50 vol %, barely coherent.

Figure 3 shows the effects of chalk on the me-

chanical properties. As expected, PS is hardened and embrittled by the chalk. Young's modulus  $E$  is increased, and the maximal tension, i.e., the tensile strength  $\sigma_m$ , as well as the elongation at break  $\epsilon_b$  and the impact strength  $a$  are decreased.

#### PS/BR

The blends PS/BR yielded morphologies as shown in Figure 1(a), with irregular domains of BR on the same scale as the chalk aggregates in Figure 2. The rubber domains proved insoluble in all solvents, evidently due to crosslinking during mixing, while the PS matrix was soluble.



**Figure 5** Types of morphology of filled blends: thermoplastic (white) elastomer (shaded) filler (black); (a) separate domains, (b) core-shell, (c) core-double-shell structure.

Figure 4 shows the mechanical effects. BR softens the PS, decreasing the modulus  $E$  and the tensile strength  $\sigma_m$ . The elongation at break  $\epsilon_b$  is increased markedly at low BR contents, with a maximum of  $\epsilon_b = 11\%$  at 10 vol % of BR. But the impact strength  $a$  is scarcely improved.

#### PS/BR/Chalk

Two alternatives exist for the morphology of filled blends PS/BR/chalk, if it is controlled by interaction energies [Fig. 5(a), (b)]. If the chalk prefers PS, the chalk and BR should form separate domains [Fig. 5(a)], and if it prefers BR, combined core-shell domains should be formed [Fig. 5(b)]. The core-shell morphology in Figure 5(b) is reminiscent of the HIPS morphology in Figure 1(b).

The pictures in Figure 6 show the observed morphologies of blends PS/BR/chalk that contain BR and chalk in equal shares. The chalk is always embedded in BR, which corresponds to the core-shell morphology in Figure 5(b). The magnifications in Figure 7 show the core-shell morphology in more detail. They also reveal a slight complication: some chalk aggregates are primarily impregnated with PS

and then surrounded by BR. This corresponds to the core-double-shell morphology indicated in Figure 5(c).

The core-shell domains of the blends PS/BR/chalk are similar in size and character to the HIPS

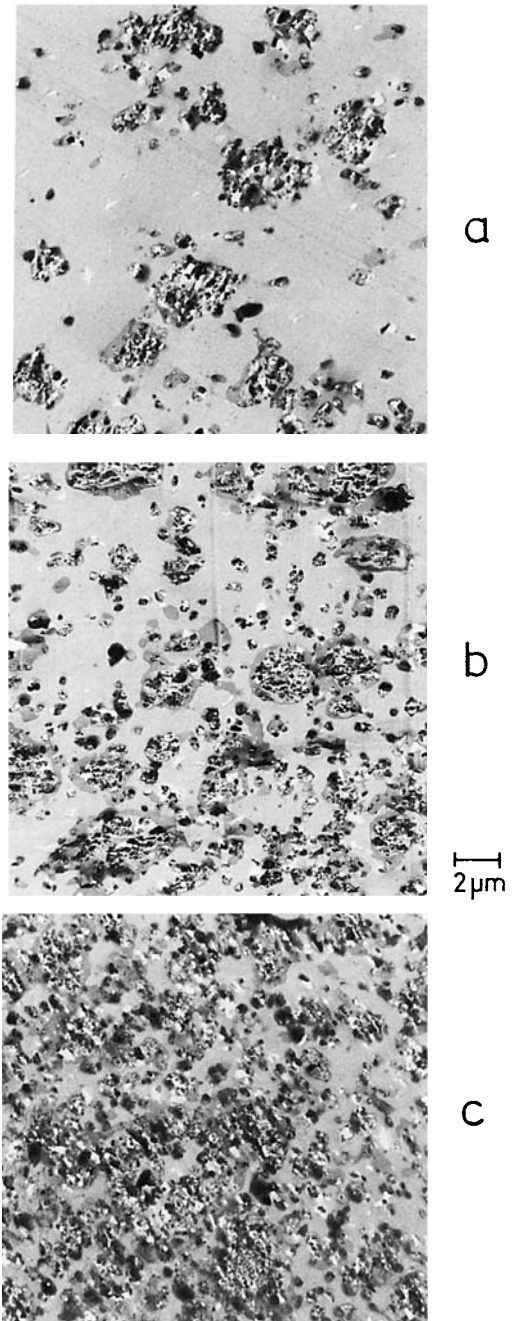


**Figure 6** Morphologies of filled blends PS/BR/chalk with equal contents of BR and chalk, (a) 10, (b) 20, (c) 30 vol % each.

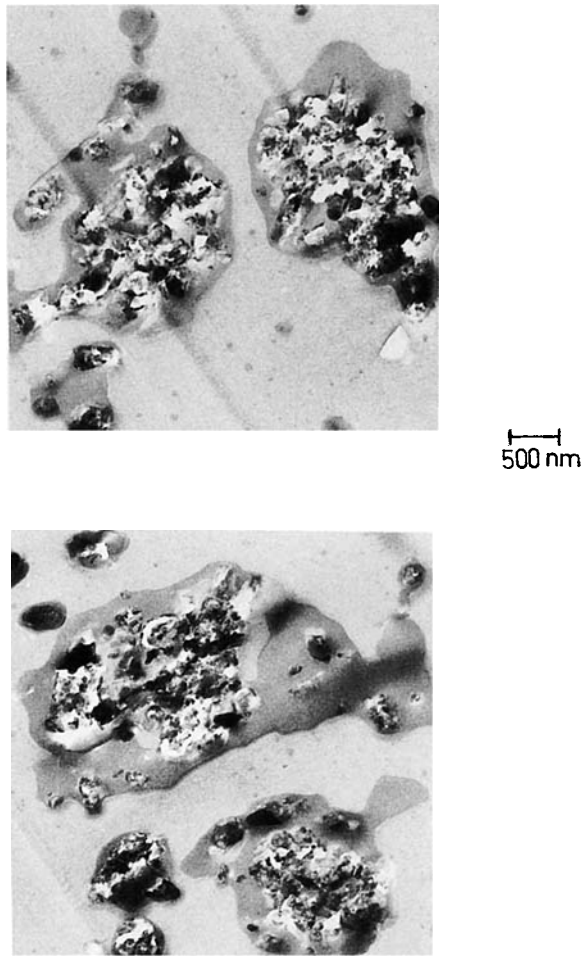


Figure 7 Magnifications from Figure 6.

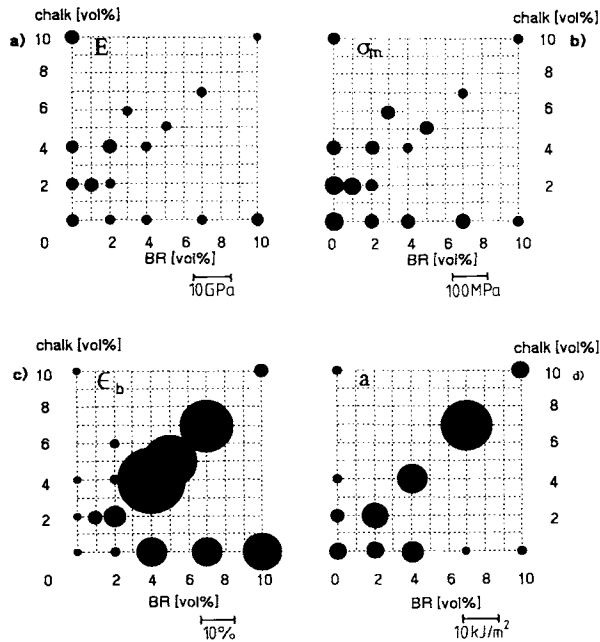


Figure 9 Filled blends PS/BR/chalk, as in Figure 8, but for smaller contents of BR and chalk.

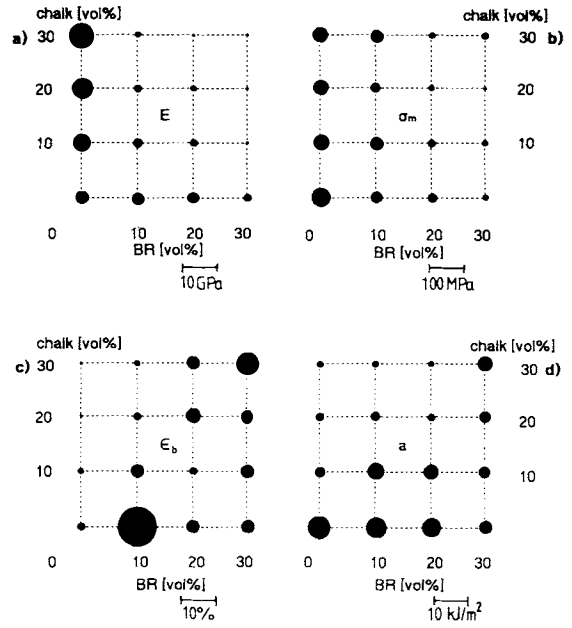


Figure 8 Filled blends PS/BR/chalk: (a) modulus  $E$ , (b) maximum stress  $\sigma_m$ , (c) elongation at break  $\epsilon_b$ , and (d) impact resistance  $a$ . The indicated bar translates the diameters of the points into the measured values.

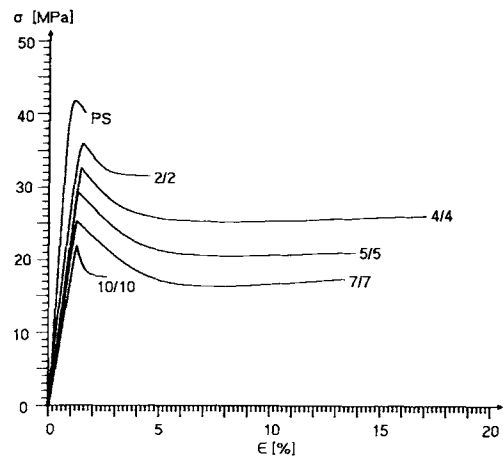
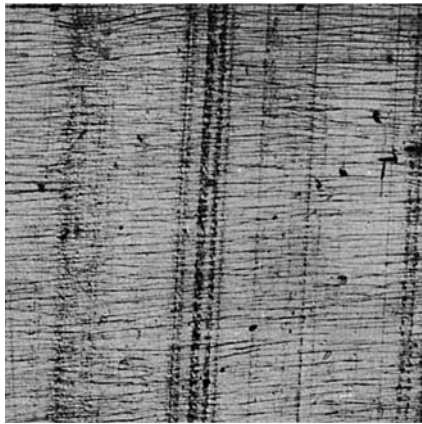
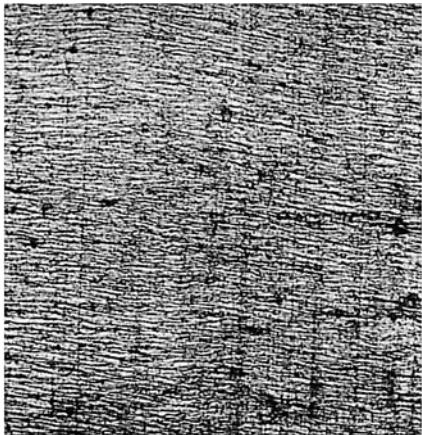


Figure 10 Stress-strain curves of filled blends PS/BR/chalk with the indicated contents of BR and chalk (vol %).

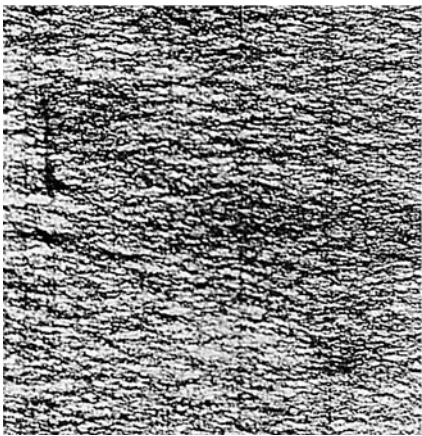


a



b

100  $\mu\text{m}$

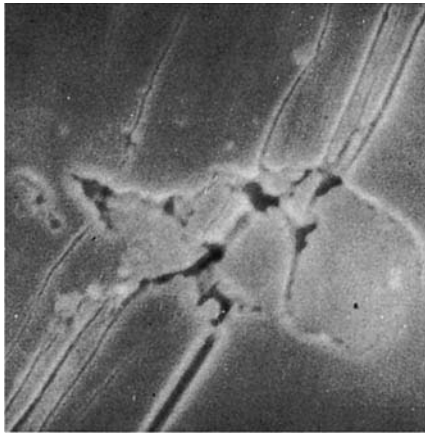


c

**Figure 11** Light microscopy: Crazes in (a) PS, (b) PS/BR<sub>2</sub>/chalk<sub>2</sub> vol %, (c) PS/BR<sub>4</sub>/chalk<sub>4</sub> vol %.



10  $\mu\text{m}$



1  $\mu\text{m}$

**Figure 12** Scanning electron microscopy: crazes on a polished surface of a filled blend PS/BR<sub>4</sub>/chalk<sub>4</sub> vol %, and a magnification of a broken chalk aggregate.



3  $\mu\text{m}$

**Figure 13** Transmission electron microscopy: crazes in a filled PS/BR<sub>4</sub>/chalk<sub>4</sub> vol % blend.

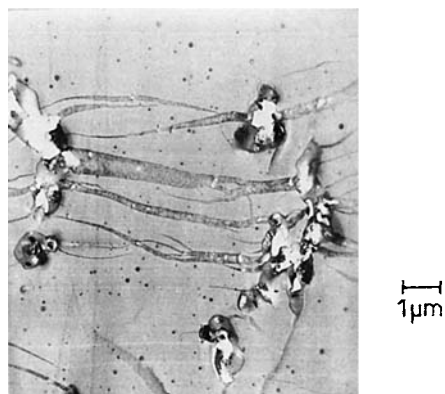


**Figure 14** Magnifications of Figure 13: (a) crazes connecting domains, (b) domain BR/chalk with lips of BR being pulled into crazes.

domains in Figure 1(b), from which they differ in two respects: (1) the core is made of a chalk aggregate instead of PS subdomains, and (2) the shell consists of homopolymer chains BR, instead of graft copolymer chains BR-g-S.

The mechanical data of blends PS/BR/chalk are compiled in Figure 8. (Note that the diameters of the data points in Figs. 8 and 9 are proportional to the measured values.)

#### Modulus $E$ and Tensile Strength $\sigma_m$

The hardening effect of chalk disappears quickly as BR is added. Most of the filled blends PS/BR/chalk are softer than PS. Evidently, the BR dominates the modulus  $E$  [Fig. 8(a)] because of the core-shell morphology: The BR shell makes the chalk core mechanically "invisible." As usual, the tensile strength  $\sigma_m$  [Fig. 8(b)] is less informative.

#### Elongation at Break $\epsilon_b$ and Impact Strength $a$

In principle,  $\epsilon_b$  and  $a$  are most informative, since they indicate the transition from brittle to ductile

failure. But Figures 8(c) and 8(d) are disappointing. None of the blends PS/BR/chalk is ductile. Yet, it turned out that the grid used in Figure 8 was simply too coarse. The grid in Figure 9 is finer, ranging only up to 10 vol % of BR and chalk. As is seen in Figures 9(c) and 9(d), there are pronounced maxima in  $\epsilon_b$  and  $a$  at low concentrations. Figure 10 shows the stress-strain curves. The most ductile blend, i.e., PS/BR/chalk (4/4 vol %), has a fairly high tensile strength,  $\sigma_m = 33$  MPa, combined with a remarkable elongation at break,  $\epsilon_b = 18\%$ , which must be compared to  $\sigma_{max} = 43$  MPa and  $\epsilon_b < 2\%$  of PS.

#### Micromechanics

PS crazes visibly, with well-defined crazes.<sup>7,12</sup> PS filled with chalk did not craze, being too brittle, while the blends PS/BR and the filled blends PS/BR/chalk exhibited, in the concentration range of 2–10 vol % of BR and chalk, pronounced stress whitening due to multicrazing. The micromechanics of the filled blends PS/BR/chalk were studied using different microscopic methods and different test specimens.

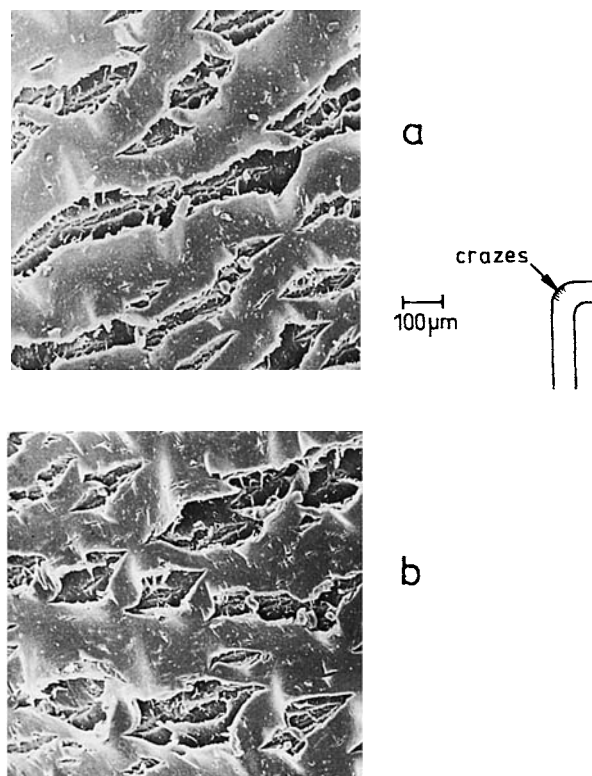


**Figure 15** Cracks in test bars of filled blends PS/BR/chalk with (a) 2 vol %, (b) 4 vol % each of BR and chalk, after bending by  $90^\circ$ .



Thin sections, 20  $\mu\text{m}$  thick, were crazed and studied by TLM while still under tension. Thin sections were necessary because the tensile test bars were not transparent enough. There should be no marked difference between crazing in the thick test bars and in the thin sections (unless the sections are ultrathin, i.e.,  $\ll 1 \mu\text{m}$ ). At least in the case of pure PS (which is sufficiently transparent), the same craze patterns were observed with both types of specimen. Figure 11(a) shows the familiar craze pattern of PS, with extremely sharp, straight, well-separated crazes. With BR and chalk added, the crazes are closer together and no longer straight [Figs. 11(b) and 11(c)].

SEM and TEM analyses were carried out using crazed test bars of blends PS/BR/chalk. The surfaces of the bars were studied with SEM and their interiors with TEM, in ultrathin sections (70 nm thick). Representative pictures are shown in Figures 12–14. They are complementary to Figure 11, showing the craze pattern on a much finer scale.

In Figures 12 and 13, most crazes start from BR/chalk domains. Some domains initiate more than one craze, on either side. Another common feature in the SEM and TEM micrographs is that the crazes starting from one domain usually do not end at another domain. Instead, they end somewhere in the PS matrix. The magnification in Figure 14(a) shows an exception, i.e., crazes that do connect different domains. These crazes are thicker than the other crazes. The high magnification in Figure 14(b) reveals a detail of craze initiation: the BR shell around the chalk particle is deformed by the crazes and pulled into them, in the form of lips.

But there are also differences between the SEM and TEM pictures. The surface crazes in Figure 12

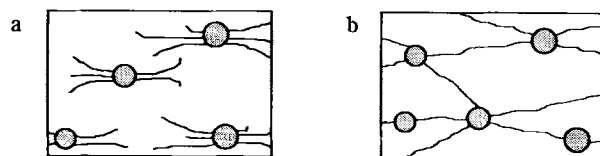


**Figure 17** Multicrazing (a) about isolated domains, and (b) in an interconnected craze network.

are straight and fairly open while the internal crazes in Figure 13 are bent and mostly very thin. Also, the magnification in Figure 12(b) shows a broken chalk aggregate that has dewetted from the matrix, which is not observed in Figure 13. TEM deserves more credit, because SEM shows surfaces that were possibly harmed while being polished. In this process, crazes may have been widened, aggregates broken up, and interfaces disconnected.

An impressive characteristic of the blends PS/BR/chalk with low contents of BR/chalk was that they could be bent easily without breaking. As indicated in Figure 15, bending (by 90 degrees) leads to crazing on the outside of the bend. SEM is particularly suited to investigate these crazes which are in a very late stage. The SEM pictures in Figure 15 show, on a coarse scale, that the crazes have turned into cracks or, rather, into wide gaps. This stage is stable only in bent, not in drawn, test bars. The multicrazing patterns have turned into a coarse pattern of only a few dominant crazes, but there are still enough of them to permit bending without fracture.

PS itself broke right away in these bending tests, due to one long, disastrous crack. But the cracks in the blend with 2 vol % each of BR and chalk are short [Fig. 15(a)], and they are even shorter in the

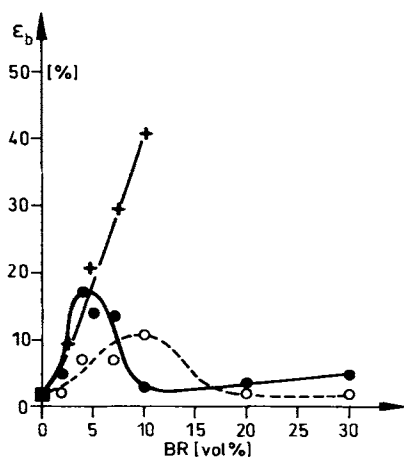


**Figure 16** Elongation at break of blends PS/BR/chalk (●), blends PS/BR (○), and HIPS (+), as a function of the BR content.

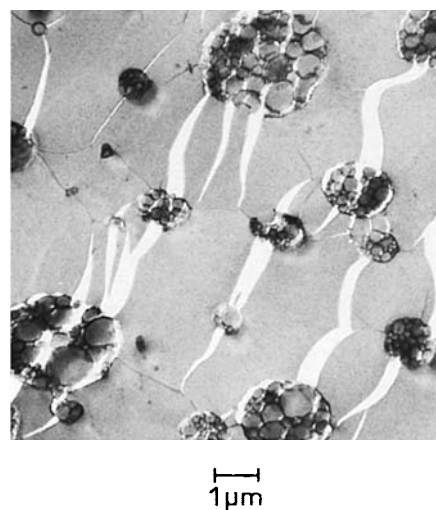


**Figure 18** Craze network in drawn HIPS.

blend with 4 vol % each [Fig. 15(b)]. It is important to emphasize that the cracks avoid each other; they do not align to form one long, disastrous crack that would destroy the sample.

## CONCLUSIONS

PS can be toughened considerably by adding surprisingly small amounts of BR and chalk. The architecture of the BR/chalk domains [Fig. 5(b),(c)] is reminiscent of that of the salami domains in HIPS [Fig. 1(b)], and the toughening mechanism by multicrazing is also apparently similar (Fig. 13).

At low concentrations of BR, the blends PS/BR/chalk are even competitive. This is demonstrated in Figure 16, in terms of the elongation at break  $\epsilon_b$  which is equal to that of HIPS. At higher concentrations of BR, 5–10 vol %, however, HIPS is even more toughened (and, of course, also softened) by intensified multicrazing, while the filled blends go back to brittle fracture. The blends PS/BR/chalk are thus good substitutes for “hard,” but not “soft,” HIPS grades.

The difference seems to be rooted in the multicraze patterns at different BR concentrations. The blends PS/BR/chalk proved in this study that they can develop multicrazing as long as they contain not too many BR/chalk domains, so that the crazes do not move straightaway from one domain to the next. This pattern of unconnected craze centers is indicated in Figure 17(a). But at higher BR concentrations, all domains will be connected by crazes, as indicated in Figure 17(b). In such a craze network, the domains cavitate and deform considerably, whereby they absorb much energy. HIPS is known to craze and deform easily in this manner,<sup>13,14</sup> as shown in Figure 18. But the filled blends, with their domains having rigid chalk aggregates in the core, cannot deform sufficiently. At higher concentrations of BR/chalk, therefore, they react brittly.

Financial support from the Bundesminister für Wirtschaft through the Arbeitsgemeinschaft Industrieller Forschungsvereinigungen (AIF, No. 8868) is gratefully acknowledged.

## REFERENCES

1. C. B. Bucknall, *Toughened Plastics*, Applied Science Publishers, London 1977; *Adv. Polym. Sci.*, **27**, 121 (1978).
2. A. Echte, F. Haaf, and J. Hambrecht, *Angew. Chem.*, **93**, 372 (1981).
3. A. Echte, *Angew. Makromol. Chem.*, **58/59**, 175 (1977).
4. G. Riess and P. Gaillard, in *Polymer Reaction Engineering—Influence of Reaction Engineering on Polymer Properties*, K. H. Reichert, W. Geiseler Eds., Hanser, Munich 1983, p. 221.
5. W. Retting, *Angew. Makromol. Chem.*, **58/59**, 133 (1977).
6. G. H. Michler, B. Hamann, and J. Runge, *Angew. Makromol. Chem.*, **180**, 169 (1990).
7. G. H. Michler, *Kunststoff-Mikromechanik: Morphologie, Deformations- und Bruchmechanismen*, Hanser, Munich, 1992, Chap. 9.
8. R. P. Sheldon, *Composite Polymeric Materials*, Applied Science Publishers, London 1982, p. 44.
9. D. M. Bigg, *Polym. Compos.*, **8**, 115 (1987).
10. L. E. Nielsen, *Mechanical Properties of Polymers*, Reinhold, New York, 1962, Chap. 6.
11. D. Braun, M. Klein, and G. P. Hellmann, *Polym. Compos.*, to appear.
12. R. P. Kambour, *J. Polym. Sci., Macromol. Rev.*, **7**, 1 (1973).
13. R. J. Seward, *J. Appl. Polym. Sci.*, **14**, 852 (1970).
14. G. H. Michler and K. Gruber, *Plaste Kautsch.*, **23**, 496 (1976).

Received May 26, 1995

Accepted November 1, 1995